Optical and neural anisotropy in peripheral vision

Len Zheleznyak
The Institute of Optics, University of Rochester, Rochester, NY, USA
Center for Visual Science, University of Rochester, Rochester, NY, USA
Flaum Eye Institute, University of Rochester, Rochester, NY, USA

Antoine Barbot
Center for Visual Science, University of Rochester, Rochester, NY, USA
Flaum Eye Institute, University of Rochester, Rochester, NY, USA

Atanu Ghosh
Center for Visual Science, University of Rochester, Rochester, NY, USA
Flaum Eye Institute, University of Rochester, Rochester, NY, USA

Geunyoung Yoon
The Institute of Optics, University of Rochester, Rochester, NY, USA
Center for Visual Science, University of Rochester, Rochester, NY, USA
Flaum Eye Institute, University of Rochester, Rochester, NY, USA

Optical blur in the peripheral retina is known to be highly anisotropic due to nonrotationally symmetric wavefront aberrations such as astigmatism and coma. At the neural level, the visual system exhibits anisotropies in orientation sensitivity across the visual field. In the fovea, the visual system shows higher sensitivity for cardinal over diagonal orientations, which is referred to as the oblique effect. However, in the peripheral retina, the neural visual system becomes more sensitive to radially-oriented signals, a phenomenon known as the meridional effect. Here, we examined the relative contributions of optics and neural processing to the meridional effect in 10 participants at 0°, 10°, and 20° in the temporal retina. Optical anisotropy was quantified by measuring the eye's habitual wavefront aberrations. Alternatively, neural anisotropy was evaluated by measuring contrast sensitivity (at 2 and 4 cyc/deg) while correcting the eye's aberrations with an adaptive optics vision simulator, thus bypassing any optical factors. As eccentricity increased, optical and neural anisotropy increased in magnitude. The average ratio of horizontal to vertical optical MTF (at 2 and 4 cyc/deg) at 0°, 10°, and 20° was 0.96 ± 0.14, 1.41 ± 0.54 and 2.15 ± 1.38, respectively. Similarly, the average ratio of horizontal to vertical contrast sensitivity with full optical correction at 0°, 10°, and 20° was 0.99 ± 0.15, 1.28 ± 0.28 and 1.75 ± 0.80, respectively. These results indicate that the neural system's orientation sensitivity coincides with habitual blur orientation. These findings support the neural origin of the meridional effect and raise important questions regarding the role of peripheral anisotropic optical quality in developing the meridional effect and emmetropization.

Introduction

In an optically well-corrected eye, foveal image quality is typically isotropic. Bright daylight conditions cause the pupil to constrict to approximately 2–3 mm in diameter (Watson & Yellott, 2012), producing a nearly aberration-free point spread function on the retina

Citation: Zheleznyak, L., Barbot, A., Ghosh, A., & Yoon, G. (2016). Optical and neural anisotropy in peripheral vision. *Journal of Vision*, *16*(5):1, 1–11, doi:10.1167/16.5.1.

doi: 10.1167/16.5.1 Received October 20, 2015; published March 1, 2016 ISSN 1534-7362

(Castejon-Mochon, López-Gil, Benito, & Artal, 2002; Thibos, Hong, Bradley, & Cheng, 2002). Due to the minimal wavefront aberrations within the typical pupil, the point spread function is largely isotropic. However, as the pupil increases, wavefront aberrations play an increasingly important role in determining the eye's optical quality.

The neural visual system has developed mechanisms to partially compensate for optically-induced visual impairment. Neural adaptation to blur has been demonstrated to improve visual performance in both short-term (Mon-Williams, Tresilian, Strang, Kochlar, & Wann, 1998) and long-term (Artal et al., 2004; Sabesan & Yoon, 2010; Sawides et al., 2010) exposure to optical aberrations. While most studies have been limited to the fovea, neural adaptation to blur in the parafovea has recently been observed (Mankowska, Aziz, Cufflin, Whitaker, & Mallen, 2012; Venkataraman, Winter, Unsbo, & Lundström, 2015).

The angular region in which the wavefront aberrations are constant, i.e., the isoplanatic patch, is limited to approximately 1 degree of visual field for a 6-mm pupil (Bedggood, Daaboul, Ashman, Smith, & Metha, 2008). Thus, optical isotropy is limited to the central fovea. Many studies (Atchison & Scott, 2002; Jaeken, Lundström, & Artal, 2011; Lundström, Gustafsson, & Unsbo, 2009; Mathur, Atchison, & Scott, 2008; Navarro, Moreno, & Dorronsoro, 1998) have observed the field dependence of the eye's wavefront aberrations. Off-axis wavefront aberrations—dominated by astigmatism and coma due to light's path through an elliptical pupil and tilted optical elements (e.g., cornea and lens)—result in a highly anisotropic point spread function. Furthermore, peripheral optical quality may be directly relevant to the visual system's development such as eye growth and myopia progression (Mathur, Atchison, & Charman, 2009a, 2009b; Mutti et al., 2011).

Perception is also influenced by the anisotropies inherent to the neural visual system such as the oblique effect, in which contrast sensitivity is preferentially higher for horizontally and vertically oriented gratings as compared to oblique orientations (Campbell, Kulikowski, & Levinson, 1966; Essock, 1990). The oblique effect has been shown to be of mostly neural origin, as confirmed with physiology (Hubel & Wiesel, 1959), functional magnetic resonance imaging (fMRI; Furmanski & Engel, 2000; Kamitani & Tong, 2005; Sasaki et al., 2006) and psychophysical studies bypassing the eye's optics using laser interference fringes (Campbell et al., 1966; Mitchell, Freeman, & Westheimer, 1967) or adaptive optics (Murray et al., 2010). However, Murray et al. (2010) have shown that habitual optical aberrations may impact the orientation-dependent sensitivity in the fovea.

In the periphery, the oblique effect yields to the meridional effect, in which visual performance is preferentially superior for radially, as opposed to azimuthally, aligned stimuli. The meridional effect has been demonstrated for contrast sensitivity (Banks, Sekuler, & Anderson, 1991; Pointer & Hess, 1989), resolution (Atchison, Mathur, & Varnas, 2013; Rovamo, Virsu, Laurinen, & Hyvärinen, 1982; Wang, Thibos, & Bradley, 1997), Vernier acuity (Yap, Levi, & Klein, 1987) and phase discrimination (Bennett & Banks, 1987, 1991) tasks. For instance, Banks et al. (1991) found that peripheral contrast sensitivity (10° nasal visual field, 4 cyc/deg, 1.5-mm pupil) for horizontally aligned gratings was greater by approximately a factor of 2, as compared to vertically aligned gratings. However, these results were obtained under nonideal optical conditions, in that field-dependent astigmatism was uncorrected in the peripheral retina during vision testing. Previous work contains evidence both for (Banks et al., 1991; Rovamo et al., 1982; Venkataraman, Winter, Rosén, & Lundström, 2016; Yap et al., 1987) and against (Cheney, Thibos, & Bradley, 2015) the hypothesis that neural mechanisms form the basis for the meridional effect. Therefore, a motivation for this study was to further investigate the basis of the meridional effect (optical vs. neural) by examining the interaction of optical and neural anisotropies in peripheral vision.

We hypothesized that long-term exposure to anisotropic blur in the peripheral retina may impact the neural anisotropy of the meridional effect. To test this hypothesis, we evaluated observers' peripheral optical quality and the impact of grating-orientation on neural contrast sensitivity in the nasal visual field. In addition, we assessed the influence of foveal refractive error on peripheral optical and neural anisotropy. The results of this study may be of clinical relevance to the field of myopia progression, in which the role of peripheral vision is an active and controversial topic of research. To quantify the eye's optical anisotropy, retinal image quality was computed from the wavefront aberrations measured across the visual field with a Shack–Hartmann wavefront sensor. Anisotropy of the visual system's neural sensitivity was assessed using an adaptive optics vision simulator to bypass the eye's optics and simultaneously measure optically-corrected contrast sensitivity across the visual field for horizontally- and vertically-aligned gratings.

Methods

Subjects

Ten subjects with normal vision participated in this study (two females; age range: 20–31 years, average: 26.7 ± 4.1 years). All subjects had no history of ocular

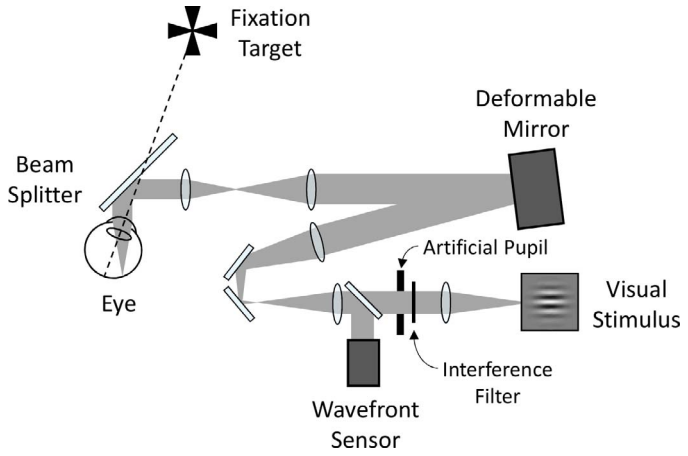

Figure 1. Simplified schematic diagram of the experimental apparatus (adaptive optics vision simulator, AOVS).

pathology and were normally sighted. All optical and psychophysical measurements were performed monocularly in the right eye, with the fellow eye occluded with an eye patch. Subjects' refractive error ranged from −5.5 to +2.0 D (average: −2.1 ± 2.7 D). Subjects' higher order RMS ranged from 0.19 to 0.54 μm (average: 0.32 ± 0.11 μm) over a 5.8-mm pupil. Subjects were cyclopleged with tropicamide (1%) to dilate the pupil and paralyze accommodation during the experiment. This research was approved by the University of Rochester Research Review Board, and all procedures involving human subjects were in accordance with the tenets of the Declaration of Helsinki. Informed consent was obtained from all subjects prior to participation in the study.

Experimental protocol

Optical and neural anisotropy were assessed at retinal eccentricities of 0° (fovea), 10°, and 20° in the temporal retina (i.e., nasal visual field). Wavefront aberrations were measured with a Shack–Hartmann wavefront sensor at each retinal location. In addition, contrast sensitivity was measured at each retinal location separately for horizontal and vertically aligned gratings at and 4 cyc/deg. Therefore, the ratio of sensitivity to horizontal and vertical gratings defined the magnitude of neural anisotropy. An adaptive optics vision simulator (AOVS) allowed us to bypass any optical factors by correcting all monochromatic and polychromatic aberrations during contrast sensitivity measurement.

Adaptive optics vision simulator

Optical quality and visual performance were assessed using the AOVS, illustrated in a simplified schematic in Figure 1. The AOVS consisted of a fixation target, a deformable mirror (ALPAO DM97, Montbonnot, France) to correct subjects' wavefront aberrations, a custom-built Shack–Hartmann wavefront sensor to measure the wavefront aberrations, an artificial pupil, and a visual stimulus. A Maltese cross (1° diameter) served as the fixation target. The visual stimulus was a modified digital light processor (Sharp XR-10X, Abeno-ku, Osaka, Japan) operating at 8 bits and with 1024 × 768 resolution. The display was Gamma-correction calibrated with a PR-650 SpectraScan Colorimeter (Photo Research, Chatsworth, CA) and subtended 3.9° × 2.9° (each pixel subtended approximately 0.23 arcminutes). A narrow-band interference filter transmitting 632.8 ± 5 nm was used in the AOVS to provide a quasimonochromatic stimulus. The AOVS was operated in continuous closed loop at approximately 8 Hz. An 840 ± 20 nm superluminescent diode was used for wavefront sensing. Head movements were stabilized with a dental impression bite bar mounted to translation stages. A camera imaging subjects' pupils was used to maintain pupil alignment.

Assessing optical anisotropy

The Shack–Hartmann wavefront sensor of the AOVS captured the optical aberrations at each retinal location (0°, 10°, and 20° temporal retina). The wavefront aberrations were defined using Zernike coefficients computed over a 6.0 mm diameter circular pupil. To emulate best-corrected habitual optical quality, the foveal lower-order aberrations (defocus and astigmatism) were subtracted from the wavefront aberrations at all eccentricities.

The light source for wavefront sensing was an 840 ± 20 nm super luminescent diode (15 $\mu W/cm^2$ at the pupil). Due to the significant difference in wavelength between the wavefront sensor device and the center of the visible spectrum, it was necessary to correct for the eye's longitudinal chromatic aberration before calculating optical quality. Therefore, a through-focus simulation of retinal image quality was performed with each subject's foveal wavefront to determine the optimal defocus correction using a custom-made MATLAB program. Area under the two-dimensional modulation transfer function (MTF) from 0 to 60 cyc/deg was the metric used in the simulation to determine optimal defocus in the fovea. The defocus value which maximized foveal retinal image quality was subsequently added to the aberrations at 10° and 20° to mimic habitual optical quality. In other words, the defocus value used to calculate the MTF in the periphery was the sum of the measured wavefront and the foveal correction. This method was intended to mimic the best-corrected habitual optical quality across the retina.

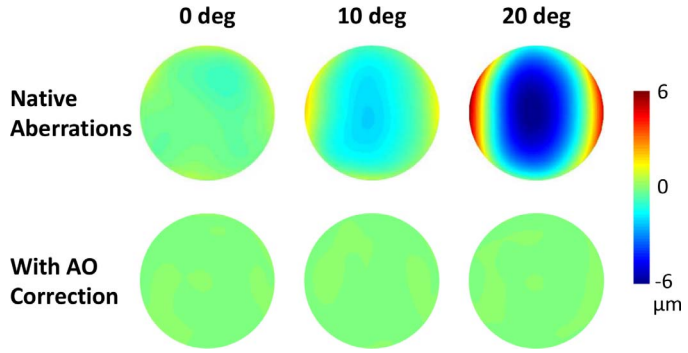

Figure 2. Wavefront aberrations (for one subject at 0°, 10°, and 20° eccentricities with (bottom row) and without (top row) AO correction.

From the resulting wavefront aberration corrected for foveal refractive error and wavefront-sensing chromatic aberration, the two-dimensional MTF was calculated (Goodman, 2005). The MTF was computed at each retinal eccentricity using an elliptical pupil with a 5.8-mm diameter major axis and a minor axis of cosine(eccentricity) × 5.8 mm (5.8, 5.71, and 5.45 mm diameter at 0°, 10°, and 20° retinal eccentricities, respectively). Individual optical anisotropy was computed for 2 and 4 cyc/deg spatial frequencies and was defined as the ratio of MTFs for horizontal to vertical gratings at each retinal location.

Assessing neural anisotropy

Contrast sensitivity was measured for horizontal and vertical sinusoidal luminance gratings (2 and 4 cyc/deg) at each retinal location (0°, 10°, and 20° temporal retina) using a two-alternative forced-choice detection method (yes–no paradigm). The stimulus consisted of a Gabor patch (1.5° full-width at half-maximum) presented for 150 ms. Each experimental block consisted of two interleaved QUEST (Watson & Pelli, 1983) staircases (40-trials each). Contrast thresholds were obtained from each staircase as the contrast resulting in 75% correct-response rate. Six threshold measurements were obtained and averaged for each retinal location, grating orientation, and spatial frequency. Individual contrast sensitivity anisotropy was computed at each eccentricity and for each spatial frequency by dividing the horizontal contrast sensitivity thresholds by the vertical contrast sensitivity thresholds.

Although the AOVS allowed aberration-free measurements, it resulted in a restricted field of view. The stimulus size was limited at all eccentricities by the field of view of the AOVS and angular extent of the DMD within the projector. Ideally, stimulus size would have been adjusted according to the cortical magnification factor, which equates the size of the cortical representation for stimuli at different eccentricities (Carrasco & Frieder, 1997; Harvey & Dumoulin, 2011; Kitterle, 1986; Rovamo & Virsu, 1979; Strasburger, Rentschler, & Jüttner, 2011; Virsu & Rovamo, 1979). Importantly, compensating for cortical magnification does not eliminate qualitative differences in neural processing between foveal and peripheral vision (Kitterle, 1986; Strasburger et al., 2011). The lack of cortical magnification correction in this experiment likely led to poorer visual performance in the periphery, making any direct comparison between eccentricities difficult. Nevertheless, the lack of cortical magnification should have not influenced sensitivity differences to horizontal and vertical gratings at a given eccentricity, and therefore had minor impact on our conclusions.

Statistical analysis

Two-way, repeated-measures ANOVAs were computed to assess the impact of eccentricity and spatial frequency on the MTF and contrast sensitivity horizontal : vertical ratios. All post-hoc comparisons were made using paired Student's *t* tests.

Results

Optical performance of the AOVS

The monochromatic stimulus ensured the absence of longitudinal and transverse chromatic aberrations, which may preferentially degrade contrast for horizontal and vertical gratings. Continuous closed-loop performance of the AOVS was aberration-free, with a residual wavefront RMS over a 6-mm pupil of approximately 0.05 μm, consistent with previous studies from our lab (Sabesan, Ahmad, & Yoon, 2007; Sabesan & Yoon, 2009; Sabesan, Zheleznyak, & Yoon, 2012). Figure 2 illustrates an example of wavefront aberrations at 0°, 10°, and 20° eccentricities both with and without AO correction for one subject. The corresponding optical anisotropy at 2 and 4 cyc/deg is shown in Table 1.

Optical anisotropy

The average change in aberrations from the fovea (0°) to the periphery (10° and 20°) is shown in Table 2. As an illustrative example, Figure 3 shows point spread functions computed from one subject's measured wavefront aberrations. As stated previously, sphere and cylinder were only corrected in the fovea. Therefore, subsequent peripheral wavefronts include the foveal

Eccentricity [degrees]	Optical anisotropy (MTF ratio)			
	Native aberrations		With AO correction	
	2 cyc/deg	4 cyc/deg	2 cyc/deg	4 cyc/deg
0	0.979	0.991	1.001	1.002
10	1.438	2.596	1.000	1.000
20	3.959	5.519	1.001	1.003

Table 1. Optical anisotropy for one subject (corresponding to wavefront aberrations shown in Figure 2) for the case of native aberrations and with the AO correction.

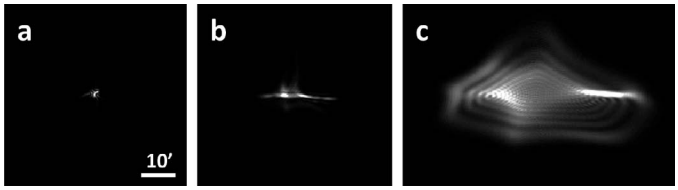

Figure 3. Point spread functions for one subject at (a) 0°, (b) 10°, and (c) 20° in the temporal retina. The scale bar corresponds to 10 arcminutes and all point spread functions are normalized in intensity.

spherocylindrical correction, similar to habitual viewing conditions.

MTF values of horizontal and vertical gratings for all retinal eccentricities are shown in Figures 4a and 4b, for 2 and and 4 cyc/deg, respectively. MTF values for 0°, 10°, and 20° eccentricities are denoted by square, circle, and triangle symbols respectively. Data points above the dashed equality line indicate optical anisotropy, wherein horizontal grating contrast is higher than vertical grating contrast. Conversely, data points below the dashed line indicate higher contrast for vertical gratings as compared to horizontal gratings.

At 2 cyc/deg, average horizontal MTF was 0.89 ± 0.05, 0.86 ± 0.07, and 0.79 ± 0.18 at 0°, 10°, and 20° eccentricities, respectively, whereas vertical MTF was 0.91 ± 0.04, 0.71 ± 0.16, and 0.52 ± 0.20. At 4 cyc/deg, average horizontal MTF was 0.69 ± 0.15, 0.63 ± 0.15, and 0.57 ± 0.19 at 0°, 10°, and 20° eccentricities, respectively, whereas vertical MTF was 0.74 ± 0.11, 0.49 ± 0.21, and 0.32 ± 0.17.

The inequality in horizontal and vertical MTFs increased with eccentricity for both spatial frequencies. The MTF ratios (Figure 5) of horizontal to vertical 2 cyc/deg gratings at 0°, 10°, and 20° were 0.98 ± 0.06, 1.27 ± 0.30, and 1.73 ± 0.62, respectively. The MTF ratios at 4 cyc/deg were 0.94 ± 0.19, 1.54 ± 0.70, and 2.57 ± 1.8.

A two-way, repeated-measures ANOVA on the MTF ratios showed a significant main effect of eccentricity, $F(2, 18) = 11.82$, $p = 0.0005$, but no significant main effect of spatial frequency, $F(1, 9) = 3.15$, $p = 0.11$. There was a marginal eccentricity-x-spatial frequency interaction, $F(2, 18) = 3.00$, $p = 0.075$.

At 2 cyc/deg, the MTF ratios were significantly higher than the equality line (ratio = 1) at 10° and 20° [0°: $t(1, 9) = -1.05$, $p = 0.319$; 10°: $t(1, 9) = 2.90$, $p = 0.0176$; 20°: $t(1, 9) = 3.73$, $p = 0.0047$], and were different from each other [10° vs. 0°: $t(1, 9) = 3.37$, $p = 0.008$; 20° vs. 10°: $t(1,9) = 2.80$, $p = 0.0206$; 20° vs. 0°: $t(1, 9) = 3.93$, $p = 0.0035$]. Similarly, at 4 cyc/deg, the MTF ratios were significantly above the equality line at 10° and 20° [0°: $t(1, 9) = -0.93$, $p = 0.375$; 10°: $t(1, 9) = 2.43$, $p = 0.038$; 20°: $t(1, 9) = 2.76$, $p = 0.022$], and differed from each other [10° vs. 0°: $t(1, 9) = 3.00$, $p = 0.015$; 20° vs. 10°: $t(1, 9) = 2.65$, $p = 0.0266$; 20° vs. 0°: $t(1, 9) = 2.95$, $p = 0.0163$].

In addition, we found that the MTF ratios were not well-correlated with foveal refractive error across eccentricities. The correlation coefficient between refractive error and MTF ratios at 0°, 10°, and 20° was $r = 0.16$, 0.15, and 0.48 at 2 cyc/deg and 0.20, 0.17, and −0.10 at 4 cyc/deg.

Neural anisotropy

Contrast sensitivity for horizontal and vertical gratings for all retinal eccentricities is shown in Figures 6a and 6b, for 2 and 4 cyc/deg, respectively. Contrast sensitivity values for 0°, 10°, and 20° eccentricities are denoted by square, circle, and triangle symbols, respectively. Data points above the dashed equality line indicate neural anisotropy, wherein contrast sensitivity is higher for horizontal gratings as compared to vertical gratings. Conversely, data points below the dashed line

Eccentricity [degrees]	Δ Sphere [D]	Δ Cylinder [D]	Δ Cylinder axis [degrees]	Δ HORMS [μm]	Δ Horizontal coma [μm]	Δ Spherical aberration [μm]
10	−0.24 ± 0.16 ($p = 0.001$)	−0.61 ± 0.31 ($p = 0.245$)	−3.1 ± 13.9 ($p = 0.518$)	0.28 ± 0.07 ($p = 0.112$)	−0.14 ± 0.12 ($p = 0.003$)	0.00 ± 0.07 ($p = 0.986$)
20	−0.47 ± 0.52 ($p = 0.018$)	−1.22 ± 0.49 ($p = 0.000$)	−1.4 ± 13.5 ($p = 0.767$)	0.42 ± 0.12 ($p = 0.001$)	−0.31 ± 0.17 ($p = 0.000$)	0.01 ± 0.07 ($p = 0.584$)

Table 2. Average ± standard deviation of change in wavefront aberrations from 0° to 10° and 20° retinal eccentricities for a 6.0-mm circular pupil. p-values refer to paired Student's t test.

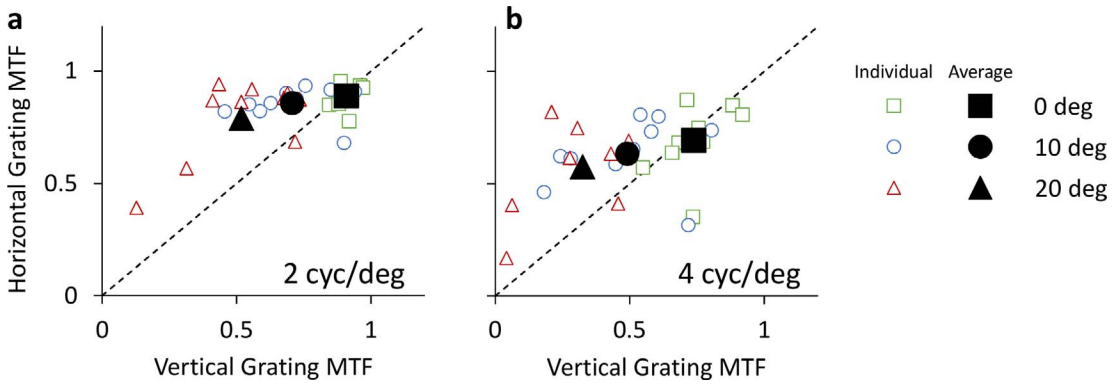

Figure 4. Optical anisotropy of habitual viewing: MTF of horizontal and vertical gratings for 2 and 4 cyc/deg (a and b, respectively). Retinal eccentricities of 0°, 10°, and 20° are denoted by square, circle, and triangle symbols, respectively. Individual data is denoted by small unfilled symbols, whereas subject average data is denoted by large filled symbols.

indicate higher contrast sensitivity for vertical gratings as compared to horizontal gratings.

At 2 cyc/deg, average horizontal contrast sensitivity was 37.6 ± 14.5, 14.8 ± 5.2, and 7.0 ± 2.4 at 0°, 10°, and 20° eccentricities, respectively. The corresponding vertical contrast sensitivity was 35.7 ± 10.6, 11.4 ± 4.0, and 4.8 ± 2.0. At 4 cyc/deg, average horizontal contrast sensitivity was 55.4 ± 43.8, 17.2 ± 15.9, and 5.9 ± 5.8 at 0°, 10°, and 20° eccentricities. The corresponding vertical contrast sensitivity was 58.6 ± 42.9, 15.3 ± 17.3, and 2.7 ± 1.5.

As illustrated in Figure 7, the inequality in horizontal and vertical contrast sensitivity increased with eccentricity for both spatial frequencies. The contrast sensitivity ratio of horizontal to vertical 2 cyc/deg gratings at 0°, 10°, and 20° was 1.04 ± 0.18, 1.32 ± 0.26, and 1.60 ± 0.68, respectively. The contrast sensitivity ratios at 4 cyc/deg were 0.94 ± 0.09, 1.25 ± 0.31, and 1.90 ± 0.91, respectively.

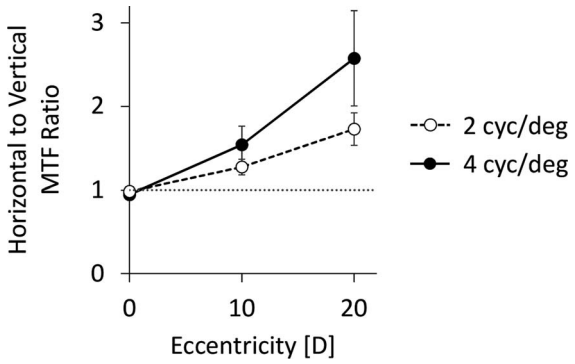

Figure 5. Average ratios of horizontal to vertical MTF values as a function of retinal eccentricity. Dashed line with unfilled symbols denotes 2 cyc/deg, and solid line with filled symbols denotes 4 cyc/deg. Dotted gray line denotes a unity ratio, implying equal horizontal and vertical MTF values. Error bars represent standard error.

A two-way repeated-measures ANOVA on the contrast sensitivity ratios showed a significant main effect of eccentricity, $F(2, 18) = 10.37$, $p = 0.001$, without significant main effect of spatial frequency, $F(1, 9) = 0.175$, $p = 0.686$, or eccentricity-*x*-spatial frequency interaction, $F(2, 18) = 1.43$, $p = 0.265$. At 2 cyc/deg, the contrast sensitivity ratios were significantly higher than the equality line (ratio = 1) at 10° and 20° [0°: $t(1, 9) = 0.633$, $p = 0.542$; 10°: $t(1, 9) = 3.80$, $p = 0.004$; 20°: $t(1, 9) = 2.80$, $p = 0.021$], and differed from each other [10° vs. 0°: $t(1, 9) = 3.39$, $p = 0.008$; 20° vs. 10°: $t(1, 9) = 1.40$, $p = 0.196$; 20° vs. 0°: $t(1, 9) = 2.89$, $p = 0.018$]. Similarly, at 4 cyc/deg, the contrast sensitivity ratio was significantly above the equality line at 10° and 20° [0°: $t(1, 9) = -2.16$, $p = 0.059$; 10°: $t(1,9) = 2.49$, $p = 0.035$; 20°: $t(1, 9) = 3.12$, $p = 0.012$], and differed from each other [10° vs. 0°: $t(1,9) = 2.99$, $p = 0.015$; 20° vs. 10°: $t(1, 9) = 2.06$, $p = 0.069$; 20° vs. 0°: $t(1,9) = 3.48$, $p = 0.007$].

In addition, the contrast sensitivity ratios were not well-correlated with foveal refractive error. The correlation coefficient between refractive error and contrast sensitivity ratios at 0°, 10°, and 20° was $r = 0.23$, 0.06, and −0.39 at 2 cyc/deg and −0.43, 0.02, and 0.07 at 4 cyc/deg.

Neural versus optical anisotropy

Figure 8 illustrates the average contrast sensitivity ratio as a function of the average MTF ratio for all eccentricities at 2 (filled symbols) and 4 (hollow symbols) cyc/deg. The coefficient of determination (R^2) between the average contrast sensitivity ratio and MTF ratio at 2 and 4 cyc/deg was 0.99 and 1.00, respectively. The slope of a linear regression between average contrast sensitivity ratio and MTF ratio at 2 and 4 cyc/deg was 0.75 and 0.60, respectively.

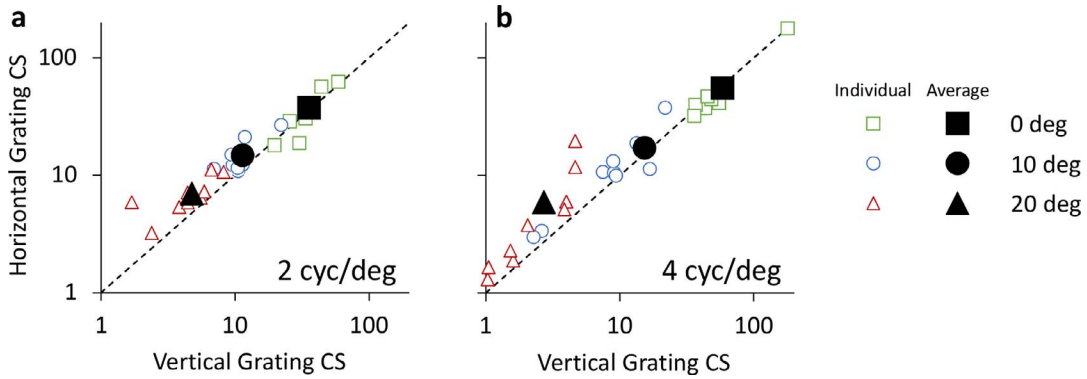

Figure 6. Contrast sensitivity (CS) of horizontal and vertical gratings for 2 and 4 cyc/deg (a and b, respectively). Retinal eccentricities of 0°, 10°, and 20° are denoted by square, circle, and triangle symbols, respectively. Individual data is denoted by small unfilled symbols, whereas subject average data is denoted by large filled symbols.

Discussion

In the present study, we quantified the degree of anisotropy of the peripheral visual system in terms of habitual optical quality and neural contrast sensitivity. The adaptive optics vision simulator enabled the disambiguation of optical and neural factors affecting visual sensitivity by correcting all optical aberrations during vision testing. We found that as retinal eccentricity increased, the anisotropy in both optical quality and neural contrast sensitivity increased in magnitude. Furthermore, the orientation-specific sensitivity of the peripheral retina coincided with higher optical contrast orientations. That is to say orientations with a deficit in neural sensitivity were also the orientations with lower habitual optical contrast. Therefore, the results of this study suggest a coupling between optical information at the retina and an allocation of neural resources to process available information at the retina.

Optical quality across the fovea is relatively constant; the human eye exhibits an isoplanatic patch of approximately 1° (Bedggood et al., 2008), which is well-matched to foveal region of highest photoreceptor density (Curcio, Sloan, Kalina, & Hendrickson, 1990). However, beyond the isoplanatic patch, optical aberrations such as astigmatism, coma, and trefoil begin to dominate optical quality, causing an anisotropic, or directional, blur (Atchison & Scott, 2002; Jaeken et al., 2011; Lundström et al., 2009; Mathur et al., 2008; Navarro et al., 1998). While the optical anisotropy of the peripheral visual system is governed by wavefront optics and the nature of light propagation, the anisotropy in sensitivity is a neural phenomenon.

Numerous studies provide evidence for neural adaptation of the adult visual system to optical quality (Artal et al., 2004; Rouger, Benard, Gatinel, & Legras, 2010; Sabesan & Yoon, 2009, 2010; Sawides et al., 2010). For example, Artal et al. (2004) found that

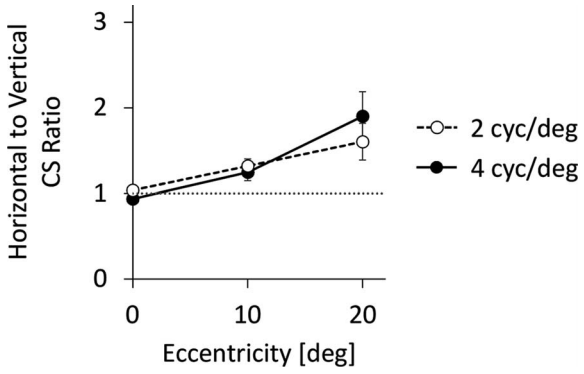

Figure 7. Average ratios of horizontal to vertical contrast sensitivity (CS) values as a function of retinal eccentricity. Dashed line with unfilled symbols denotes 2 cyc/deg, and solid line with filled symbols denotes 4 cyc/deg. Dotted gray line denotes a unity ratio, implying equal horizontal and vertical contrast sensitivity values. Error bars represent standard error.

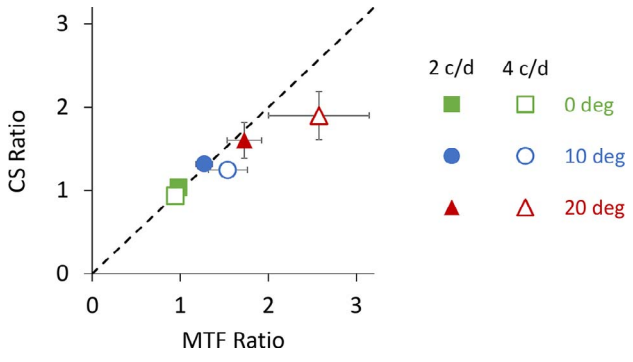

Figure 8. Average contrast sensitivity (CS) ratio versus average MTF ratio for all retinal eccentricities at 2 (filled symbols) and 4 (hollow symbols) cyc/deg. Retinal eccentricity is denoted with green, blue and red symbols for 0°, 10°, and 20° eccentricities. Dashed line indicates the equality line. Error bars represent standard error.

subjects perceived a target to be sharpest with their native orientation of the point spread function, as opposed to rotated orientations. Similarly, in optically-abnormal eyes with keratoconus, the neural visual system has been shown to compensate for long-term exposure to highly-aberrated point spread functions, resulting in improved visual acuity (Rouger et al., 2010; Sabesan & Yoon, 2010). Our findings suggest a similar relationship for peripheral vision, with the neural system being adapted to the optical quality of the peripheral retina.

Visual performance is roughly the product of the optical quality and the neural response. Each time we open our eyes, we are confronted with far more information than our visual system can effectively process, due to the high metabolic cost of cortical computations. Therefore, our visual system needs mechanisms to optimally allocate processing resources. Our findings show that optical and neural anisotropy coincide, allowing the neural visual system to avoid allocating resources to orientations with poor optical quality. We propose that neural anisotropy may come as a consequence of the eye's optical anisotropy in an effort to conserve resources. Similar mechanisms have been referred to previously as *neural insensitivity* (Chen, Artal, Gutierrez, & Williams, 2007; Sabesan & Yoon, 2009).

The present study confirms the neural origins of the meridional effect. Potential neural mechanisms responsible for our observations of anisotropy in sensitivity have been described in the literature. For instance, Banks et al. (1991) attributed the meridional effect to processes in the cortex and neuronal pooling in the retina. Physiological (Hubel & Wiesel, 1959), and more recently, fMRI (Furmanski & Engel, 2000; Kamitani & Tong, 2005; Sasaki et al., 2006) studies, have shown that analysis of orientation first occurs in the primary visual cortex (V1). In the retina, topography of ganglion cell receptive fields has been shown to affect orientation-specific visual tasks, such as contrast sensitivity (Levick & Thibos, 1982) and perceptual distortions (McGraw & Whitaker, 1999; Vera-Diaz, McGraw, Strang, & Whitaker, 2005). However, it should be noted that a recent study (Cheney et al., 2015) concluded that transverse chromatic aberration, not neural processing, accounts for the origins of the meridional effect in grating detection acuity. Specifically, Cheney et al. (2015) found that the orientation bias of detection acuity in white light was limited by transverse chromatic aberration. The discrepancy between this and the current study may be due to the differences in psychophysical tasks. For example, the detection acuity task used in the study by Cheney et al. (2015) is limited by retinal photoreceptor sampling, which is largely isotropic (Curcio et al., 1990). In contrast, in the present study, we used a detection task at relatively low spatial frequencies well below the sampling limit.

Retinal factors affecting visual anisotropy must occur beyond the photoreceptor stage in vision, due to their isotropic distribution throughout the retina. Vera-Diaz et al. (2005) concluded that elongation of ganglion cell receptive fields due to axial elongation of the ocular globe was responsible for spatial distortions. Furthermore, the degree of spatial distortion was correlated with subjects' axial length, implying radially elongated ganglion cell receptive fields. In the current study, 10 subjects participated with a moderate range of foveal refractive error (−5.5 to 2.5 D), which is well-correlated with axial length. Therefore, we would expect a relationship between refractive error and neural anisotropy. Although this study did not find a significant correlation between refractive error and neural anisotropy, this question merits further investigation with a larger sample size.

The developing visual system is, at least in part, shaped by early visual experience. For example, it has been proposed that neonatal optical quality may influence the orientation sensitivity of the neural visual system in the fovea (i.e., the oblique effect; Murray et al., 2010). While optical quality in infants is typically hyperopic (Mayer, Hansen, Moore, Kim, & Fulton, 2001; Saunders, Woodhouse, & Westall, 1995), their magnitude of higher-order wavefront aberrations has been shown to be similar to that of the adult eye (Wang & Candy, 2005). Previous studies have suggested beneficial roles for neonatal aberrations, such as cues for accommodation (Wilson, Decker, & Roorda, 2002) and the emmetropization process (Wallman & Winawer, 2004).

Eye growth has been shown to be regulated, at least in part, by the optics in the peripheral retina of infant monkeys (Smith, Hung, & Huang, 2009; Smith III, Kee, Ramamirtham, Qiao-Grider, & Hung, 2005). Peripheral hyperopia is common in axially elongated, myopic eyes (Mutti, Sholtz, Friedman, & Zadnik, 2000; Mutti et al., 2011). Conversely, emmetropic eyes typically have a myopic shift in the peripheral retina with respect to the fovea. Moreover, it has been suggested that the relationship between the blur for tangential and radial neurons may control eye growth (Charman et al., 2011). A large enough peripheral anisotropic blur may potentially trigger eye growth. However, longitudinal studies in children are needed to confirm whether meridional effect is a consequence of, or cause to, myopia development.

Multifocal contact lenses have emerged as a clinical technique to deter excessive eye growth in children by manipulating the optics in the peripheral retina (Aller & Wildsoet, 2008; Anstice & Phillips, 2011; Walline, Greiner, McVey, & Jones-Jordan, 2013). This approach is meant to create a myopic defocus in the peripheral retina without disturbing foveal vision. The present

study confirms the anisotropic nature of neural sensitivity in the peripheral retina. This should be taken into consideration in the optical design and implementation of multifocal strategies to myopia progression. For example, the ratio of radial to azimuthal contrast may impact the efficacy of multifocal strategies for myopia control.

Finally, we only measured contrast sensitivity in the temporal retina along the horizontal visual field. Based on previously published studies of optical and neural anisotropy, we expect our conclusions to hold to other retinal meridians. Future studies should expand the present work to oblique and vertical meridians in order to better characterize the relationship between optical and neural anisotropies across the entire visual field.

Conclusion

Optical and neural anisotropy of the peripheral visual system were quantified using an adaptive optics vision simulator. As eccentricity increased, the degree of optical and neural anisotropy increased in magnitude. Orientation sensitivity of the neural system coincided with visual orientations of habitually superior optically quality. These findings support the neural origin of the meridional effect and raise important questions regarding the role of peripheral anisotropic optical quality in developing the meridional effect and emmetropization.

Keywords: wavefront aberrations, anisotropy, neural adaptation, adaptive optics, peripheral retina

Acknowledgements

We would like to thank Martin Banks for his helpful comments on this manuscript. We would also like to thank Ramkumar Sabesan and Jesse Schallek for insightful discussions. This work was supported by NIH/NEI EY014999 and Research to Prevent Blindness. The authors have no financial or proprietary interests.

Commercial relationships: none.
Corresponding author: Geunyoung Yoon.
Email: yoon@cvs.rochester.edu..
Address: The Institute of Optics, Rochester, NY, USA.

References

Aller, T. A., & Wildsoet, C. (2008). Bifocal soft contact lenses as a possible myopia control treatment: a case report involving identical twins. *Clinical and Experimental Optometry*, *91*, 394–399.

Anstice, N. S., & Phillips, J. R. (2011). Effect of dual-focus soft contact lens wear on axial myopia progression in children. *Ophthalmology*, *118*, 1152–1161.

Artal, P., Chen, L., Fernández, E. J., Singer, B., Manzanera, S., & Williams, D. R. (2004). Neural compensation for the eye's optical aberrations. *Journal of Vision*, *4*(4):4, 281–287, doi:10.1167/4.4.4. [PubMed] [Article]

Atchison, D. A., Mathur, A., & Varnas, S. R. (2013). Visual performance with lenses correcting peripheral refractive errors. *Optometry & Vision Science*, *90*(11), 1304–1311.

Atchison, D. A., & Scott, D. H. (2002). Monochromatic aberrations of human eyes in the horizontal visual field. *Journal of the Optical Society of America A*, *19*(11), 2180–2184.

Banks, M. S., Sekuler, A. B., & Anderson, S. J. (1991). Peripheral spatial vision: Limits imposed by optics, photoreceptors, and receptor pooling. *Journal of the Optical Society of America A*, *8*(11), 1775–1787.

Bedggood, P., Daaboul, M., Ashman, R., Smith, G., & Metha, A. (2008). Characteristics of the human isoplanatic patch and implications for adaptive optics retinal imaging. *Journal of Biomedical Optics*, *13*(2), 024008-1–024008-7.

Bennett, P. J., & Banks, M. S. (1987). Sensitivity loss in odd-symmetric mechanisms and phase anomalies in peripheral vision. *Nature*, *326*(6116), 873–876.

Bennett, P. J., & Banks, M. S. (1991). The effects of contrast, spatial scale, and orientation on foveal and peripheral phase discrimination. *Vision Research*, *31*(10), 1759–1786.

Campbell, F., Kulikowski, J., & Levinson, J. (1966). The effect of orientation on the visual resolution of gratings. *The Journal of Physiology*, *187*(2), 427–436.

Carrasco, M., & Frieder, K. S. (1997). Cortical magnification neutralizes the eccentricity effect in visual search. *Vision Research*, *37*(1), 63–82.

Castejon-Mochon, J. F., López-Gil, N., Benito, A., & Artal, P. (2002). Ocular wave-front aberration statistics in a normal young population. *Vision Research*, *42*(13), 1611–1617.

Charman, W. N. (2011). Keeping the world in focus: how might this be achieved? *Optometry & Vision Science*, *88*, 373–376.

Chen, L., Artal, P., Gutierrez, D., & Williams, D. R. (2007). Neural compensation for the best aberration correction. *Journal of Vision*, *7*(10):9, 1–9, doi:10.1167/7.10.9. [PubMed] [Article]

Cheney, F., Thibos, L., & Bradley, A. (2015). Effect of ocular transverse chromatic aberration on detection acuity for peripheral vision. *Ophthalmic and Physiological Optics*, *35*(1), 70–80.

Curcio, C. A., Sloan, K. R., Kalina, R. E., & Hendrickson, A. E. (1990). Human photoreceptor topography. *Journal of Comparative Neurology*, *292*(4), 497–523.

Essock, E. A. (1990). The influence of stimulus length on the oblique effect of contrast sensitivity. *Vision Research*, *30*(8), 1243–1246.

Furmanski, C. S., & Engel, S. A. (2000). An oblique effect in human primary visual cortex. *Nature Neuroscience*, *3*(6), 535–536.

Goodman, J. W. (2005). *Introduction to Fourier optics*. Englewood, CO: Roberts and Company Publishers.

Harvey, B. M., & Dumoulin, S. O. (2011). The relationship between cortical magnification factor and population receptive field size in human visual cortex: Constancies in cortical architecture. *The Journal of Neuroscience*, *31*(38), 13604–13612.

Hubel, D. H., & Wiesel, T. N. (1959). Receptive fields of single neurones in the cat's striate cortex. *The Journal of Physiology*, *148*(3), 574–591.

Jaeken, B., Lundström, L., & Artal, P. (2011). Peripheral aberrations in the human eye for different wavelengths: Off-axis chromatic aberration. *Journal of the Optical Society of America A*, *28*(9), 1871–1879.

Kamitani, Y., & Tong, F. (2005). Decoding the visual and subjective contents of the human brain. *Nature Neuroscience*, *8*(5), 679–685.

Kitterle, F. L. (1986). Psychophysics of lateral tachistoscopic presentation. *Brain and Cognition*, *5*(2), 131–162.

Levick, W., & Thibos, L. (1982). Analysis of orientation bias in cat retina. *The Journal of Physiology*, *329*, 243.

Lundström, L., Gustafsson, J., & Unsbo, P. (2009). Population distribution of wavefront aberrations in the peripheral human eye. *Journal of the Optical Society of America A*, *26*(10), 2192–2198.

Mankowska, A., Aziz, K., Cufflin, M. P., Whitaker, D., & Mallen, E. A. (2012). Effect of blur adaptation on human parafoveal vision. *Investigative Ophthalmology & Visual Science*, *53*(3), 1145–1150. [PubMed] [Article]

Mathur, A., Atchison, D. A., & Charman, W. N. (2009a). Effect of accommodation on peripheral ocular aberrations. *Journal of Vision*, *9*(12):20, 1–11, doi:10.1167/9.12.20. [PubMed] [Article]

Mathur, A., Atchison, D. A., & Charman, W. N. (2009b). Myopia and peripheral ocular aberrations. *Journal of Vision*, *9*(10):15, 1–12, doi:10.1167/9.10.15. [PubMed] [Article]

Mathur, A., Atchison, D. A., & Scott, D. H. (2008). Ocular aberrations in the peripheral visual field. *Optics Letters*, *33*(8), 863–865.

Mayer, D. L., Hansen, R. M., Moore, B. D., Kim, S., & Fulton, A. B. (2001). Cycloplegic refractions in healthy children aged 1 through 48 months. *Archives of Ophthalmology*, *119*(11), 1625–1628.

McGraw, P. V., & Whitaker, D. (1999). Perceptual distortions in the neural representation of visual space. *Experimental Brain Research*, *125*(2), 122–128.

Mitchell, D. E., Freeman, R. D., & Westheimer, G. (1967). Effect of orientation on the modulation sensitivity for interference fringes on the retina. *Journal of the Optical Society of America*, *57*(2), 246–249.

Mon-Williams, M., Tresilian, J. R., Strang, N. C., Kochhar, P., & Wann, J. P. (1998). Improving vision: Neural compensation for optical defocus. *Proceedings of the Royal Society of London B: Biological Sciences*, *265*(1390), 71–77.

Murray, I. J., Elliott, S. L., Pallikaris, A., Werner, J. S., Choi, S., & Tahir, H. J. (2010). The oblique effect has an optical component: Orientation-specific contrast thresholds after correction of high-order aberrations. *Journal of Vision*, *10*(11):10, 1–12, doi:10.1167/10.11.10. [PubMed] [Article]

Mutti, D. O., Sholtz, R. I., Friedman, N. E., & Zadnik, K. (2000). Peripheral refraction and ocular shape in children. *Investigative Ophthalmology & Visual Science*, *41*, 1022–1030. [PubMed] [Article]

Mutti, D. O., Sinnott, L. T., Mitchell, G. L., Jones-Jordan, L. A., Moeschberger, M. L., Cotter, S. A., … CLEERE Study Group. (2011). Relative peripheral refractive error and the risk of onset and progression of myopia in children. *Investigative Ophthalmology & Visual Science*, *52*(1), 199–205. [PubMed] [Article]

Navarro, R., Moreno, E., & Dorronsoro, C. (1998). Monochromatic aberrations and point-spread functions of the human eye across the visual field. *Journal of the Optical Society of America A*, *15*(9), 2522–2529.

Pointer, J., & Hess, R. (1989). The contrast sensitivity gradient across the human visual field: With emphasis on the low spatial frequency range. *Vision Research*, *29*(9), 1133–1151.

Rouger, H., Benard, Y., Gatinel, D., & Legras, R. (2010). Visual tasks dependence of the neural compensation for the keratoconic eye's optical aberrations. *Journal of Optometry*, *3*(1), 60–65.

Rovamo, J., & Virsu, V. (1979). An estimation and application of the human cortical magnification factor. *Experimental Brain Research*, *37*(3), 495–510.

Rovamo, J., Virsu, V., Laurinen, P., & Hyvärinen, L. (1982). Resolution of gratings oriented along and across meridians in peripheral vision. *Investigative Ophthalmology & Visual Science*, *23*(5), 666–670. [PubMed] [Article]

Sabesan, R., Ahmad, K., & Yoon, G. (2007). Correcting highly aberrated eyes using large-stroke adaptive optics. *Journal of Refractive Surgery*, *23*(9), 947–952.

Sabesan, R., & Yoon, G. (2009). Visual performance after correcting higher order aberrations in keratoconic eyes. *Journal of Vision*, *9*(5):6, 1–10, doi:10.1167/9.5.6. [PubMed] [Article]

Sabesan, R., & Yoon, G. (2010). Neural compensation for long-term asymmetric optical blur to improve visual performance in keratoconic eyes. *Investigative Ophthalmology & Visual Science*, *51*(7), 3835–3839. [PubMed] [Article]

Sabesan, R., Zheleznyak, L., & Yoon, G. (2012). Binocular visual performance and summation after correcting higher order aberrations. *Biomedical Optics Express*, *3*(12), 3176–3189.

Sasaki, Y., Rajimehr, R., Kim, B. W., Ekstrom, L. B., Vanduffel, W., & Tootell, R. B. (2006). The radial bias: a different slant on visual orientation sensitivity in human and nonhuman primates. *Neuron*, *51*(5), 661–670.

Saunders, K. J., Woodhouse, J. M., & Westall, C. A. (1995). Emmetropisation in human infancy: Rate of change is related to initial refractive error. *Vision Research*, *35*(9), 1325–1328.

Sawides, L., Marcos, S., Ravikumar, S., Thibos, L., Bradley, A., & Webster, M. (2010). Adaptation to astigmatic blur. *Journal of Vision*, *10*(12):22, 1–15, doi:10.1167/10.12.22. [PubMed] [Article]

Smith, E. L., Hung, L. F., & Huang, J. (2009). Relative peripheral hyperopic defocus alters central refractive development in infant monkeys. *Vision Research*, *49*, 2386–2392.

Smith, E. L. III, Kee, C.-s., Ramamirtham, R., Qiao-Grider, Y., & Hung, L.-F. (2005). Peripheral vision can influence eye growth and refractive development in infant monkeys. *Investigative Ophthalmology & Visual Science*, *46*, 3965–3972. [PubMed] [Article]

Strasburger, H., Rentschler, I., & Jüttner, M. (2011). Peripheral vision and pattern recognition: A review. *Journal of Vision*, *11*(5):13, 1–82, doi:10.1167/11.5.13. [PubMed] [Article]

Thibos, L. N., Hong, X., Bradley, A., & Cheng, X. (2002). Statistical variation of aberration structure and image quality in a normal population of healthy eyes. *Journal of the Optical Society of America A*, *19*(12), 2329–2348.

Venkataraman, A. P., Winter, S., Rosén, R., & Lundström, L. (2016). Choice of grating orientation for evaluation of peripheral vision. *Optometry & Vision Science*.

Venkataraman, A. P., Winter, S., Unsbo, P., & Lundström, L. (2015). Blur adaptation: Contrast sensitivity changes and stimulus extent. *Vision Research*, *110*, 100–106.

Vera-Diaz, F. A., McGraw, P. V., Strang, N. C., & Whitaker, D. (2005). A psychophysical investigation of ocular expansion in human eyes. *Investigative Ophthalmology & Visual science*, *46*(2), 758–763. [PubMed] [Article]

Virsu, V., & Rovamo, J. (1979). Visual resolution, contrast sensitivity, and the cortical magnification factor. *Experimental Brain Research*, *37*(3), 475–494.

Walline, J. J., Greiner, K. L., McVey, M. E., & Jones-Jordan, L. A. (2013). Multifocal contact lens myopia control. *Optometry & Vision Science*, *90*, 1207–1214.

Wallman, J., & Winawer, J. (2004). Homeostasis of eye growth and the question of myopia. *Neuron*, *43*(4), 447–468.

Wang, J., & Candy, T. R. (2005). Higher order monochromatic aberrations of the human infant eye. *Journal of Vision*, *5*(6):6, 543–555, doi:10.1167/5.6.6. [PubMed] [Article]

Wang, Y.-Z., Thibos, L. N., & Bradley, A. (1997). Effects of refractive error on detection acuity and resolution acuity in peripheral vision. *Investigative Ophthalmology and Visual Science*, *38*(10), 2134–2143. [PubMed] [Article]

Watson, A. B., & Pelli, D. G. (1983). QUEST: A Bayesian adaptive psychometric method. *Perception & Psychophysics*, *33*(2), 113–120.

Watson, A. B., & Yellott, J. I. (2012). A unified formula for light-adapted pupil size. *Journal of Vision*, *12*(10):12, 1–16, doi:10.1167/12.10.12. [PubMed] [Article]

Wilson, B. J., Decker, K. E., & Roorda, A. (2002). Monochromatic aberrations provide an odd-error cue to focus direction. *Journal of the Optical Society of America A*, *19*(5), 833–839.

Yap, Y. L., Levi, D. M., & Klein, S. A. (1987). Peripheral hyperacuity: Isoeccentric bisection is better than radial bisection. *Journal of the Optical Society of America A*, *4*(8), 1562–1567.